Hindawi
Material Design & Processing Communications
Volume 2022, Article ID 7436024, 12 pages
https://doi.org/10.1155/2022/7436024

Research Article

Investigating Static Deflection of Non-Prismatic Axially Functionally Graded Beam

Walaa Mohammed Hashim,[1] **Luay S. Alansari**,[1] **Mohanad Aljanabi**,[2] **and Hassan Mansour Raheem**[1,2]

[1]*Mechanical Department, Faculty of Engineering, University of Kufa, Najaf, Iraq*
[2]*Ministry of Oil, Midland Refineries Company, Karbala Refinery, Karbala, Iraq*

Correspondence should be addressed to Hassan Mansour Raheem; enghas25@gmail.com

Received 13 March 2022; Revised 11 May 2022; Accepted 28 June 2022; Published 18 July 2022

Academic Editor: Guian Qian

In this study, the static deflection of non-prismatic axial function graded tapered beam (A-FGB) under distribution load has been analyzed using ANSYS workbench (17.2). According to a power-law model, the elastic modulus of the beam varies continuously in the axial direction of the beam. Also, the beam's geometry, i.e., width, thickness, or both width and thickness of the beam, varies linearly in the axial direction with different values of non-uniformity parameter (1, 0.5,0, −0.5, and −0.75). The effects of martial distribution, i.e., power-law index, and non-uniformity parameter on the static deflection for A-FGB with different boundary conditions, in such free-clamped, clamped-free, and simply-supported, are studied. This research deals with functionally graded materials FGMs in more than one aspect in terms of using different boundary conditions; in addition, it studies the response of the non-prismatic beam non-uniformity parameter (α); therefore, this research studies comprehensively the deflection of the beam. The results show that the increase in power-law index causes decreasing in dimensionless deflection and its rate of change depends on the supporting types of the beam and non-uniformity parameters. The variation in both width and thickness for a free-clamped axial function–graded beam gives a significant decrease in dimensionless deflection at decreasing in non-uniformity parameter, whereas the variation in thickness for clamped-free axial function graded beam gives a significant decrease in dimensionless deflection at decreasing of non-uniformity parameter.

1. Introduction

Composite materials are new materials that have a combination of mechanical properties that cannot be achieved in original or pure materials individually. Composite materials can be divided into several types according to the reinforcing material shape, such as fiber, laminate, and particles-composite. The obvious disadvantage of conventional composite materials is the discontinuity in physical and mechanical properties. To overcome this defect, functionally graded materials (FGMs) are used in several engineering applications like aerospace industries, automotive industries, defense industries, and biomedical engineering. FGMs are a type of composite materials in which the material properties are engineered to differ continuously and steadily from one surface to others to minimize discontinuity effects in properties [1–4].

Generally, beams and plates are the main structural components that can be fabricated as FGMs to improve the mechanical behaviors of such structures. In comparison, non-uniform cross-section beams are commonly used due to space limitations and advantageous construction.

Researchers studied the effects of using both variable cross-section FGMs on the static and dynamic responses, the vibration of the beam, and many applications [5–9]. The functional grade beams (FGB) can be divided into two types: varying material properties through-thickness and it is denoted as T-FGB, and varying material properties axially that are designated as A-FGB. Several studies have been carried out to study the static response of T-FGB [10–12].

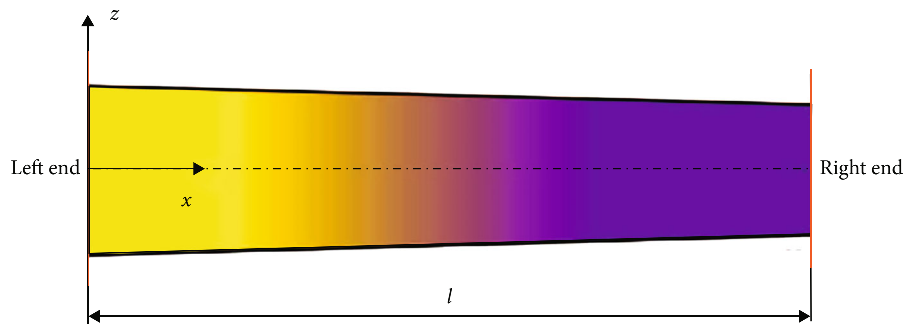

Figure 1: Mechanical and physical property distribution in the axial direction of FGB.

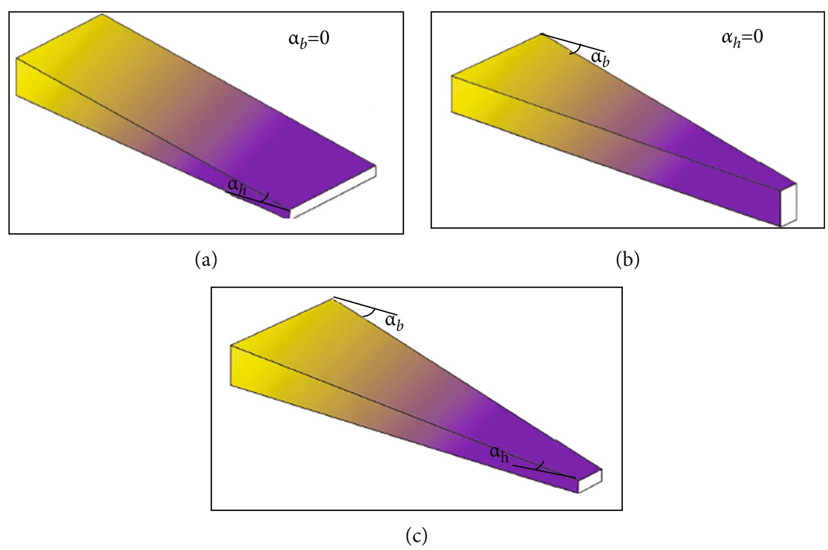

Figure 2: Three cases of non-prismatic beams studied in this work: case 1 (a) thickness variation only; case 2 (b) width variation only; case 3 (c) thickness and width variation.

Baker [13] measured the static deflection of a slender tapered cantilever beam under randomly dispersed loads for non-prismatic beams by solving the governing differential equation with the weight residual process. Lee et al. [14] investigated, experimentally and theoretically, tapered cantilever beams with a large displacement. They solved the governing differential equations numerically using Runge–Kutta method. Brojan et al. [15] calculated the deformed shape of non-prismatic cantilever beams using the generalized Ludwick law under a tipping moment. Attarnejad et al. [16] derived the displacement functions of tapered Timoshenko beams to study the free vibration by solving the governing equations of motion.

Many publications analyzed FGM structures that were subjected to different loadings and discussed the effects of the material distribution of FGM on axial and transverse displacements. Sankar [17] derived an elasticity solution for T-FGBs under a static transverse load based on Euler–Bernoulli beam theory. Kadoli et al. [18] investigated the static behavior of. FGM beams under ambient temperature using the higher-order shear deformation beam theory. Singh and Li [19] suggested a model for calculating buckling loads of non-uniform A-FGM columns. Kang and Li [20, 21] derived expressions for displacements of a nonlinear T-FGM cantilever under a transverse tip load and a tip moment. Alshorbagy et al. [22] used the finite element method to calculate the natural frequencies of both T-FGB and A-FGB considering Euler-Bernoulli beam theory. Wattanasakulpong et al. [23] used the Ritz method to study the thermal buckling and elastic vibration of T-FGB by considering the third-order shear deformation theory. Shahba et al. [24] calculated the critical loads and vibration characteristics of tapered Timoshenko A-FGB by formulating the mass and stiffness matrices considering the homogeneous solution of a uniform Timoshenko segment that was adopted from [25]. Nguyen et al. [26] studied the static analysis of tapered beam with T-FGM and A-FGM analytically under transverse load considering the Euler–Bernoulli beam theory and the principle of virtual work. Nguyen [27] used the finite element method to calculate the large displacement response of a tapered cantilever A-FGB. He studied the effects of taper type, taper ratio, and length to height ratio on the axial and transverse displacements of the beam. Padhi et al. [28] adopted the finite element principle and the first-

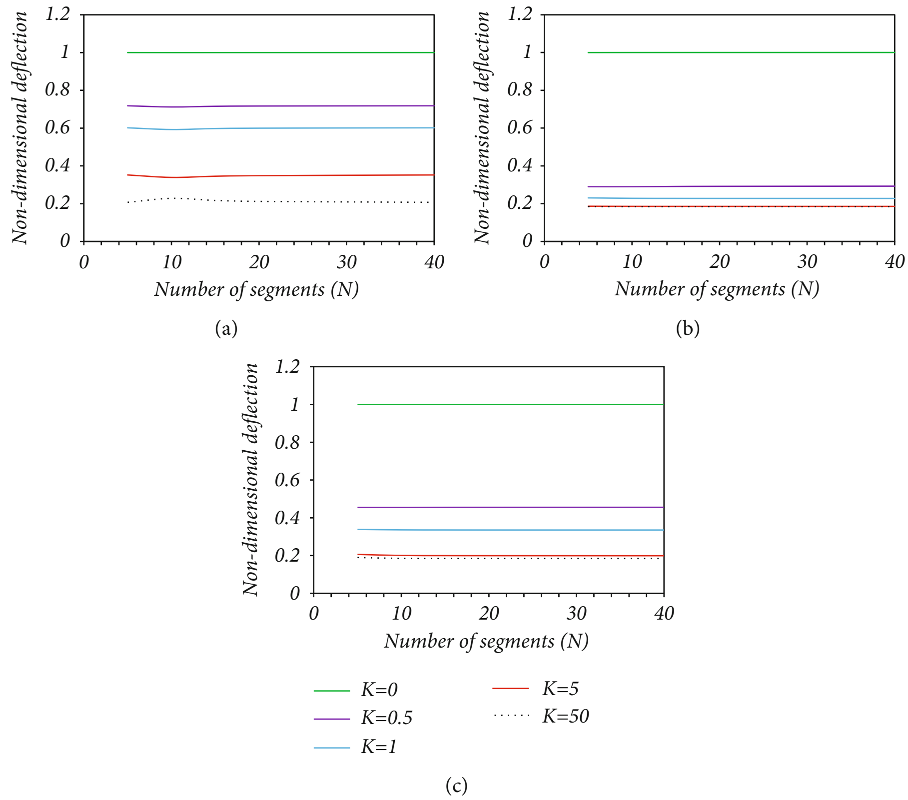

FIGURE 3: Effect of the number of segments in ANSYS A-FGB models: (a) free-clamped; (b) clamped-free; (c) simply-supported.

order shear deformation principle to study the static and dynamic behavior of a simply-supported sigmoid functionally graded ordinary beam. Rajasekaran and Khaniki [29] presented a comprehensive study on mechanical behaviors of non-homogenous non-uniform size-dependent A-FGB with different types of materials using the finite element method.

Most literature has not considered studying the effects of changing the boundary conditions, i.e., support's type of the beam, on the deflection response under load; therefore, in this study, the static deflection of tapered A-FGBs with three different boundary conditions, i.e., free-clamped, clamped-free, and simply-supported, were investigated using ANSYS workbench (version 17.2). Also, the effects of taper ratio, taper type, and power-law index on the static deflection were studied.

2. Materials and Methods

2.1. Functionally Graded Beam FGB. The mechanical properties of FGB have been distributed axially (A-FGM) as shown in Figure 1. It can be represented according to the power-law model (Equation (1)) [30]:

$$P(x) = (P_L - P_R) * \left[1 - \left(\frac{x}{l}\right)^K\right] + P_R, \tag{1}$$

where,

P_R and P_L are properties at the right and left ends of the tapered beam, respectively; K is the power-law index; l is the length of the tapered beam; and x is the distance along the length of the beam.

It is worthy to mention that the material properties are considered a ceramic on the left side of the beam, whereas it is considered a pure metal on the right side of the beam. Material properties are considered to be changed gradually in between the ends. In other words, the variation of mechanical and physical properties depends on the value of the power-law index (K) and the properties of the two parent's materials, i.e., the ceramic and metal, at the beam's ends. A beam theory was adopted to formulate the equations of this research. More information can be found in Reference [31].

2.2. Dimensions of Non-Prismatic A-FGB. In this work, three types of non-prismatic are considered. It can be represented as varying in thickness, width, or both the thickness and width of the beam. Equations (2) and (3) [26] state these variations as

$$h(x) = h_0 * \left(1 + \alpha_h * \left(\frac{x}{l}\right)\right), \tag{2}$$

$$b(x) = b_0 * \left(1 + \alpha_b * \left(\frac{x}{l}\right)\right), \tag{3}$$

where,

$h(x)$ and $b(x)$ are the thickness and width of the beam, respectively, as a function of distance (x) along the length of the beam. h_0 and b_0 are the thickness and width, respectively, of the beam at the left end. α_h and α_b are the non-

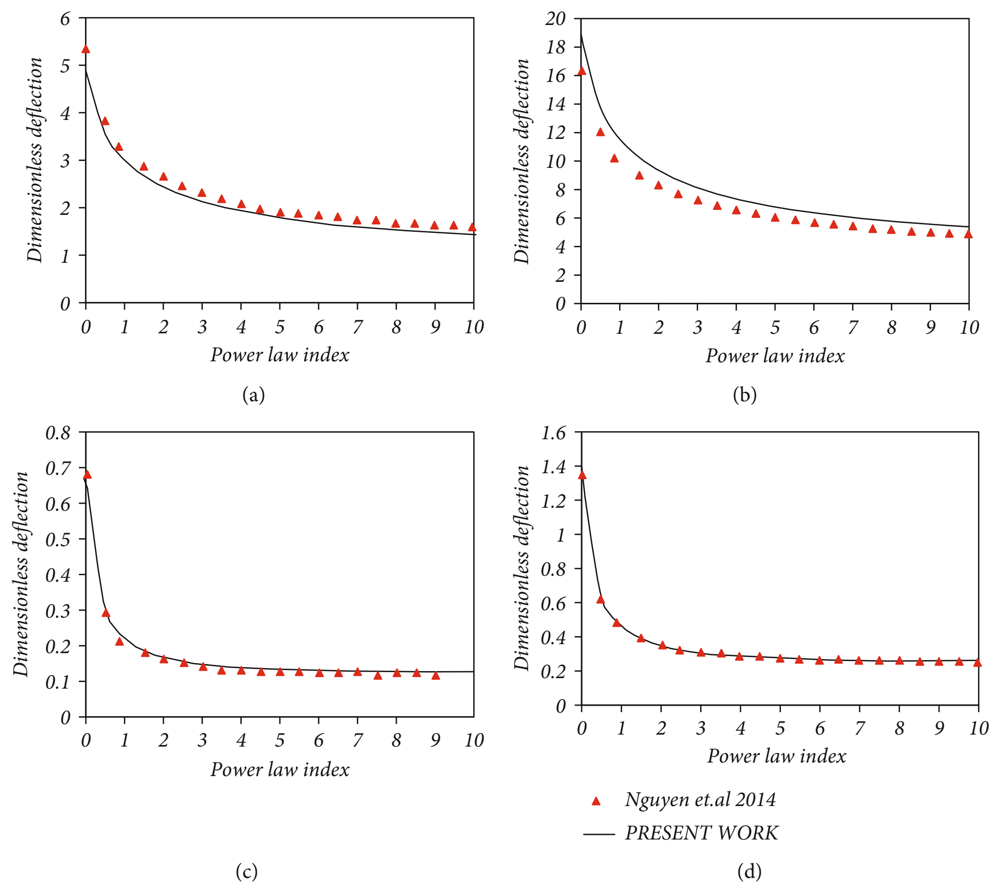

FIGURE 4: Validation of ANSYS model: (a) free-clamped A-FGB when $\alpha_b = 1$; (b) free-clamped A-FGB when $\alpha_b = -0.5$; (c) simply-supported A-FGB when $\alpha_b = 1$; and (d) simply-supported A-FGB when $\alpha_b = -0.5$.

TABLE 1: Discrepancy percentages between results of the present model and that of Nguyen et al. [26].

Non-uniformity parameter	Free-clamped A-FGB Discrepancy percentages		Simply-supported A-FGB Discrepancy percentages	
	Max.	Min.	Max.	Min.
$\alpha = 1$	12.4865	6.6504	1.0769	-9.5907
$\alpha = -0.5$	−10.2437	−14.5467	4.0751	−1.64305

uniformity parameter in thickness and width directions, respectively.

Also, the three variations that were considered in this study are as follows:

(1) Thickness variation only: The width of the beam is considered a constant, and it equals to (b_0), i.e., $\alpha_b = 0$, as shown in Figure 2(a)

(2) Width variation only: The thickness of the beam is considered a constant, and it equals to (h_0), i.e., $\alpha_h = 0$, as shown in Figure 2(b)

(3) Both width and thickness variation: Both width and thickness of the tapered beam are considered varied together with the same slope, i.e., $\alpha_h = \alpha_b$, as shown in Figure 2(c)

2.3. ANSYS Model. ANSYS workbench (version 17.2) was utilized to model the static deflection of tapered A-FGBs with three different boundary conditions, i.e., free-clamped, clamped-free, and simply-supported.

To simulate the axial variations in mechanical and physical properties, the length of the beam is divided into (N) segments, and the properties of each segment are equal to the average of start and end properties of the segment as shown in the following equation:

$$([P(x)]_{i-\text{seg.}} = \left([P_{Start}(x)]_{i-\text{seg.}} + [P_{End}(x)]_{i-\text{seg.}}\right)/2. \quad (4)$$

To examine the effects of changing the number of N segments on the static deflection of the model, a uniform A-FGB was simulated. The model was examined at different

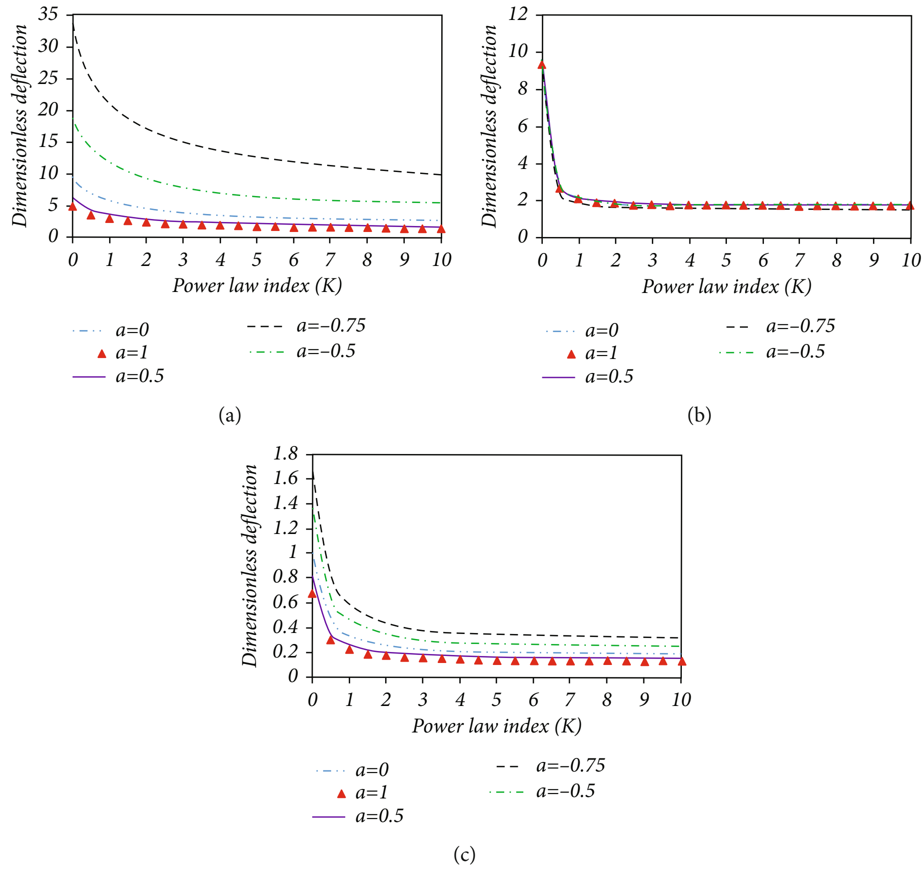

Figure 5: Effect of the power-law index (K) on the maximum deflection of A-FGB with different boundary conditions under distribution load and width variation: (a) free - clamped A-FGB; (b) clamped-free A-FGB; and (c) simply-supported A-FGB.

boundary conditions, i.e., different types of supports, in such free-clamped, clamped-free, and simply-supported, with different power-law index K. Figure 3 illustrates the number of segments N against the deflection of FGB for each type of support. The number of segments (N) does not significantly affect the results of static deflection when the number of segments (N) is greater than (10). Therefore, a model with 20 segments was adopted in this research.

To build the model, the first step in the finite element procedure is to split the domain of the model into components, i.e., discretization. The distribution of the mechanical component is called mesh elements, which join in points set of nodes [32]. The characteristics of loads and boundary conditions are considered in the model. In the current research, a static deflection is used, and a series of equations are solved using numerical analysis rather than ordinary differential equations to simulate the physical problem of the model.

Shell181 element types [32, 33] with edge element size (10 mm) are used to mesh the problem's domain, i.e., the beam. The number of elements in the non-prismatic beam is about 1300-1500, while the number of nodes is about 2000-2400, which is dependent on the non-uniformity parameters.

2.4. Validation. To ensure that the current model is accurate and valid, a comparison with available literature [26] has been carried out. Nguyen et al. [26] assumed that the elastic moduli of ceramic (left side material) and metal (right side material) are 380 GPa and 70 GPa, respectively, and the non-uniformity parameter of width variation is (1) and (−0.5).

Nguyen et al. [26] applied a uniform distribution load on the A-FGB to obtain a dimensionless deflection using the following equation:

$$W^* = w * \frac{384 * E_m * I_0}{5\,Ql^4}, \tag{5}$$

where,

(W^*) denotes the non-dimensionless transverse deflection. (w) is the transverse deflection. (E_m) is the elastic modulus of metal. (Q) is the distributed load, and (I_0) is the moment of inertial and equals to $I_0 = b_0 h_0^3/12$.

Figure 4 compares the current results of the model with those of Nguyen et al. [26] for simply-supported and free-clamped A-FGB with different values of the power-law index (K). Table 1 reports the results of this work and Nguyen et al.'s [26] study. It seems that there is an excellent agreement between the dimensionless deflections of the present model with that of Nguyen et al. [26] in the simply-supported A-FGB at non-uniformity parameters (1) and

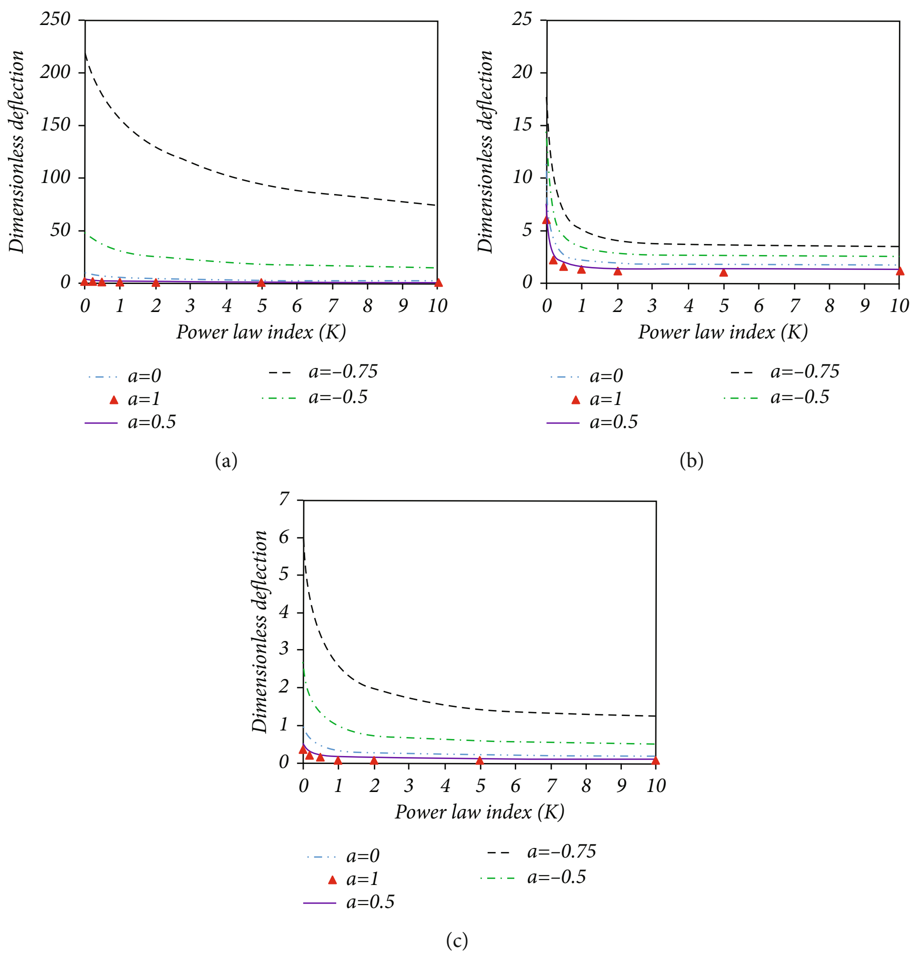

FIGURE 6: Effect of the power-law index (K) on the maximum deflection of A-FG beam with different boundary conditions under distribution load and thickness variation: (a) free-clamped A-FGB; (b) clamped-free A-FGB; and (c) simply-supported A-FGB.

(−0.5). However, the agreement between the results of the free-clamped A-FGB is less than that of a simply-supported A-FGB, but it is still acceptable.

As stated in Table 1, the discrepancy appeared in the results, but was still within the range and accepted. This can be interpreted as the beam is non-prismatic; in addition, it is a functionally graded material with different Young Modulus, and those factors have slightly affected the results in free clamped beam. However, in the case of the simply-supported beam, it is fixed on both sides, and the increase and decrease of alpha do not present significant effects on the results. The comparisons generally show similar trends and behavior to those reported results [26].

3. Results and Discussion

The elastic moduli of materials of the models are ceramic, i.e., located at the left side with 380 GPa, whereas the metal is modeled at the right side of the beam with 70 GPa. The beam's non-uniformity parameters, i.e., α_b and α_h, are considered 1, 0.5, 0, -0.5 and -0.75. In other words, when the width and thickness of the beam change together $(\alpha_h = \alpha_b = \alpha)$. The magnitude of (α) will be considered as (1, 0.5, 0, −0.5, and −0.75). The effects of non-uniformity parameters and power-law index (K) on the dimensionless deflection with different types of support of A-FGBs, i.e., free-clamped, clamped-free, and simply-supported, examine under distributed load.

3.1. Effects of Width Variation. Figure 5 states the variation of maximum dimensionless deflection due to the increase in the power-law index for different non-uniformity parameters. It is clear that when the power low index increases, the maximum dimensionless deflection decreases. This can be interpreted as increasing power low index (K) leads to an increase in the equivalent elastic modulus of A-FGB and eventually contributes to decreasing in the static deflection for all supporting types of A-FGBs.

Also, the non-uniformity parameter in the width of the beam significantly affects the deflection in the free-clamped beam (Figure 5(a)) in comparison with its influences on other types of supports (Figures 5(b) and 5(c)).

However, when the non-uniformity parameter in width decreases, i.e., $\alpha = -0.75$, the maximum dimensionless deflection increases. This influence can be explained by considering the position of the clamped end. If the position of the clamped end is on the side of a smaller elastic modulus, i.e., right side, the maximum dimensionless deflection is expected, while if the position of the clamped end is on the

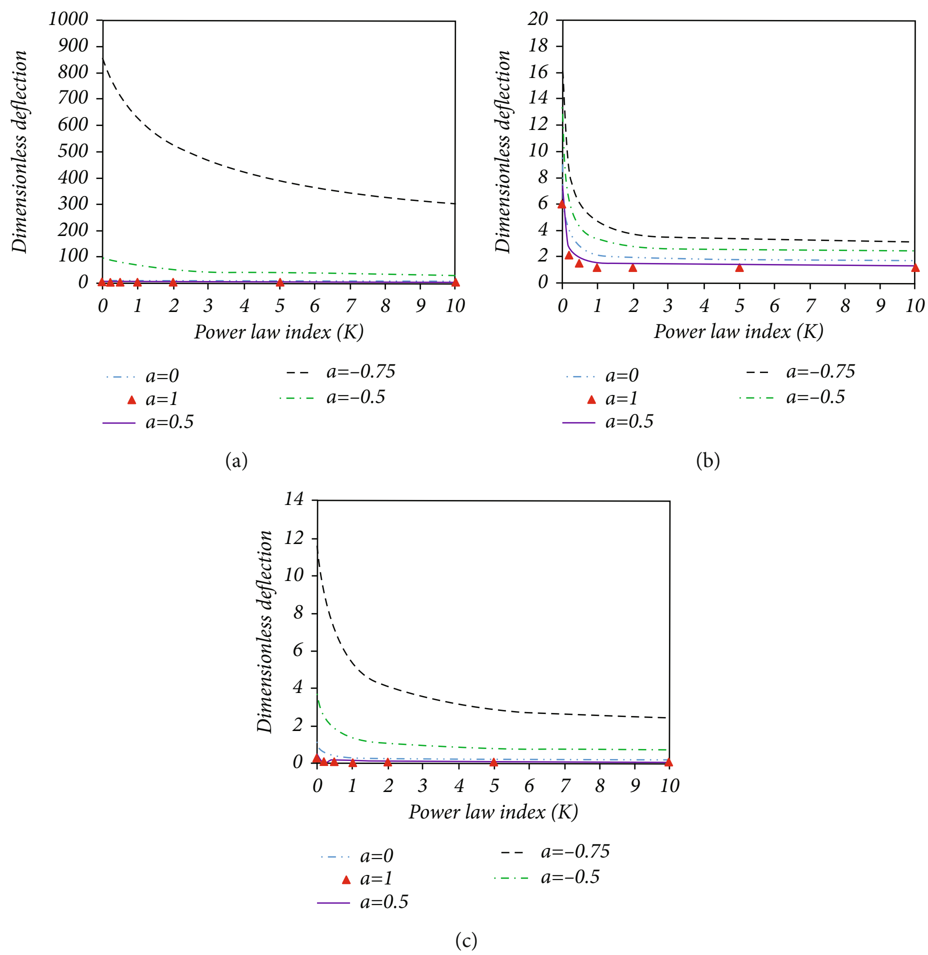

Figure 7: Effects of the power-law index (K) on the maximum deflection of A-FG beam with different boundary conditions under distribution load and width and thickness variations: (a) free-clamped A-FGB; (b) clamped-free A-FGB; and (c) simply-supported A-FGB.

side of the larger elastic modulus, i.e., left side, the maximum dimensionless deflection will decrease. In addition, the geometry of the beam, i.e., changing in width, affects the relationship between the applied distribution load and the area (length ∗ width). The distribution load is represented as the pressure applied to the area. In this case, when the non-uniformity parameter increases, the area will increase, and the load on the right side will be greater than the load on the left side of the beam.

It can reversibly occur if the non-uniformity parameter decreases, the area (length ∗ width) will decrease, and the load on the right side will be smaller than the load on the left side of the beam. Generally, the maximum dimensionless deflection decreases when the non-uniformity parameter increases for the same power-law index for any supporting type.

3.2. Effects of Thickness Variation. Figure 6 shows the effects the of non-uniformity parameter of thickness variation, α_h, on the maximum dimensionless deflection at different power-law indexes and supporting types. In this scenario, the width of the beam is constant; therefore, the applied distribution load is constant along the beam, but the moment of inertia and elastic modulus change along the length of the beam. The changing of the moment of inertia is due to the thickness variation along the length of the beam.

It is obvious that, for all supporting types, the maximum dimensionless deflection increases, while the non-uniformity parameter decreases (α_h) and the rate of increase depends on the supporting types. The maximum rate of dimensionless deflection appears in free-clamped support (Figure 6(a)) in comparison with other supports Figures 6(b) and 6(c). The main factors that affected the maximum dimensionless deflection and its rate of change are the distribution of elastic moduli, the position of the clamped end, and the change in moment of inertia.

3.3. Effects of Both Width and Thickness Variations. Figure 7 depicts the influences of the variation of width and thickness together at the same rate on the maximum dimensionless deflection at different power-law indexes. With increasing K, the maximum dimensionless deflection decreases for all supporting types as has been observed with other scenarios. Also, the increase in non-uniformity parameters leads to a decrease in maximum dimensionless deflection. The rate of change in maximum dimensionless deflection in free-clamped A-FGB (Figure 7(a)) is greater than in clamped-free and simply-supported A-FGBs.

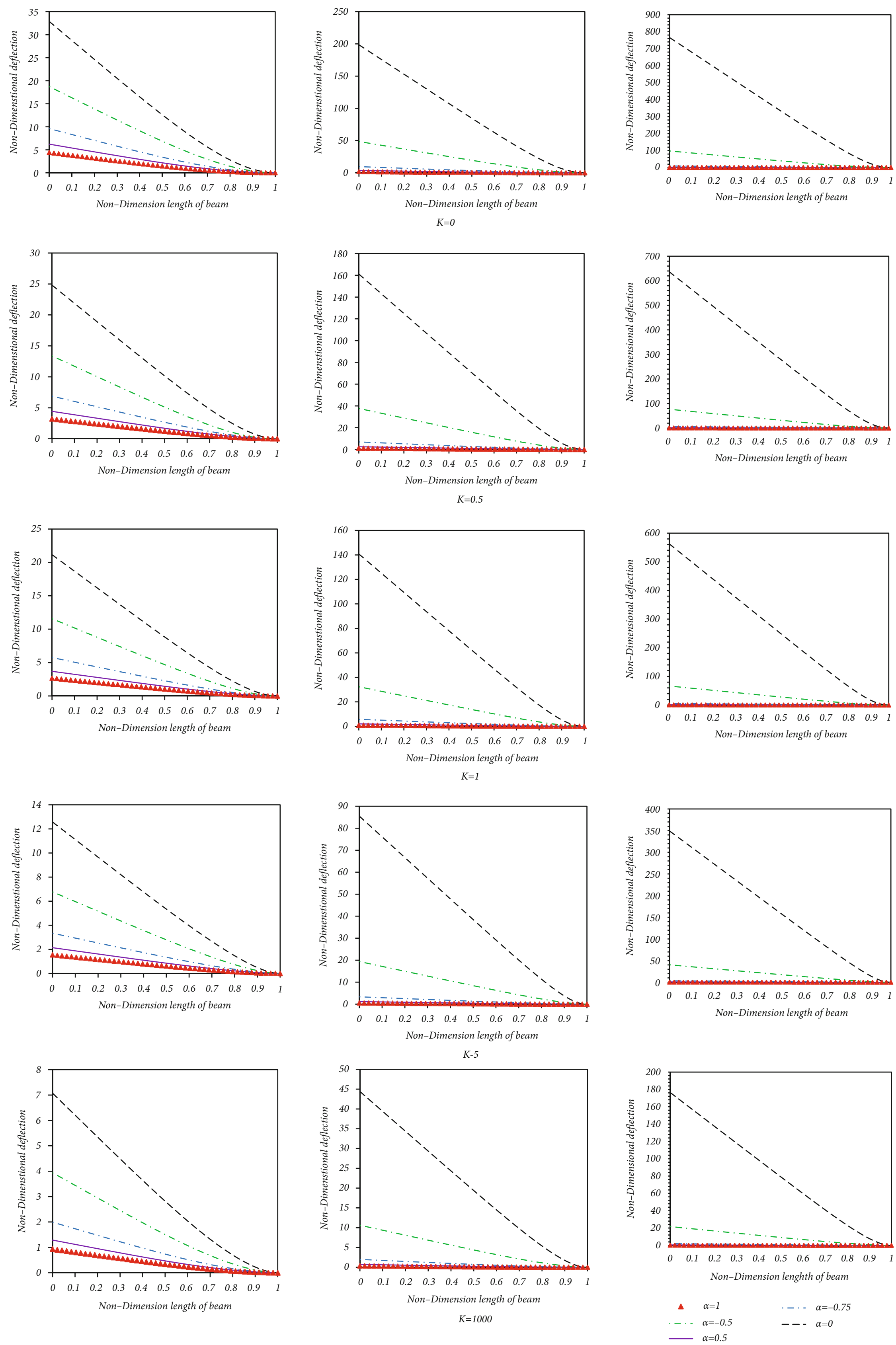

FIGURE 8: Static non-dimensional deflection along the length of free-clamped A-FGB under distribution load with different non-uniformity parameters.

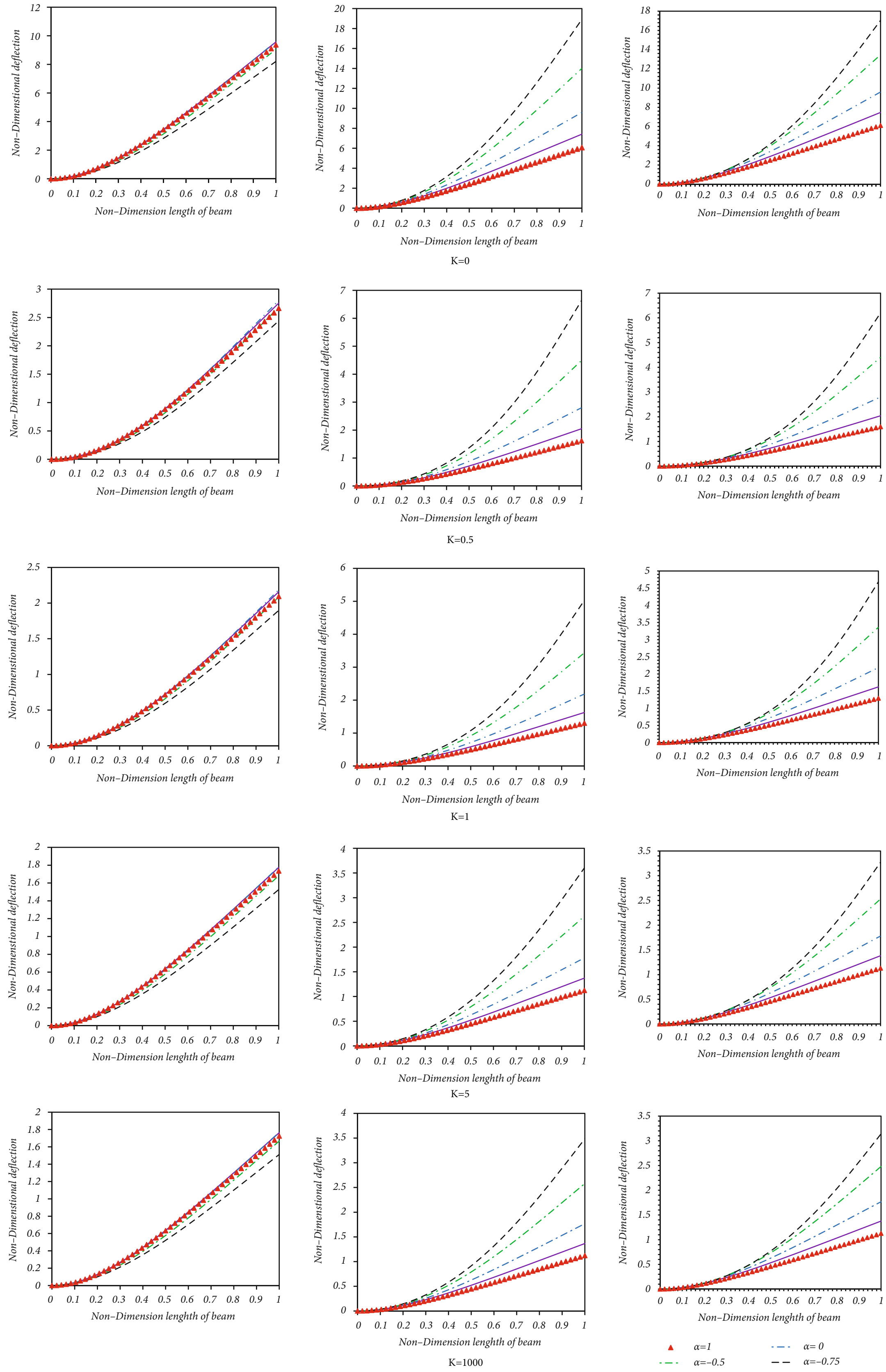

Figure 9: Static nondimensional deflection along the length of clamped-free A-FGB under distribution load with different non-uniformity parameters.

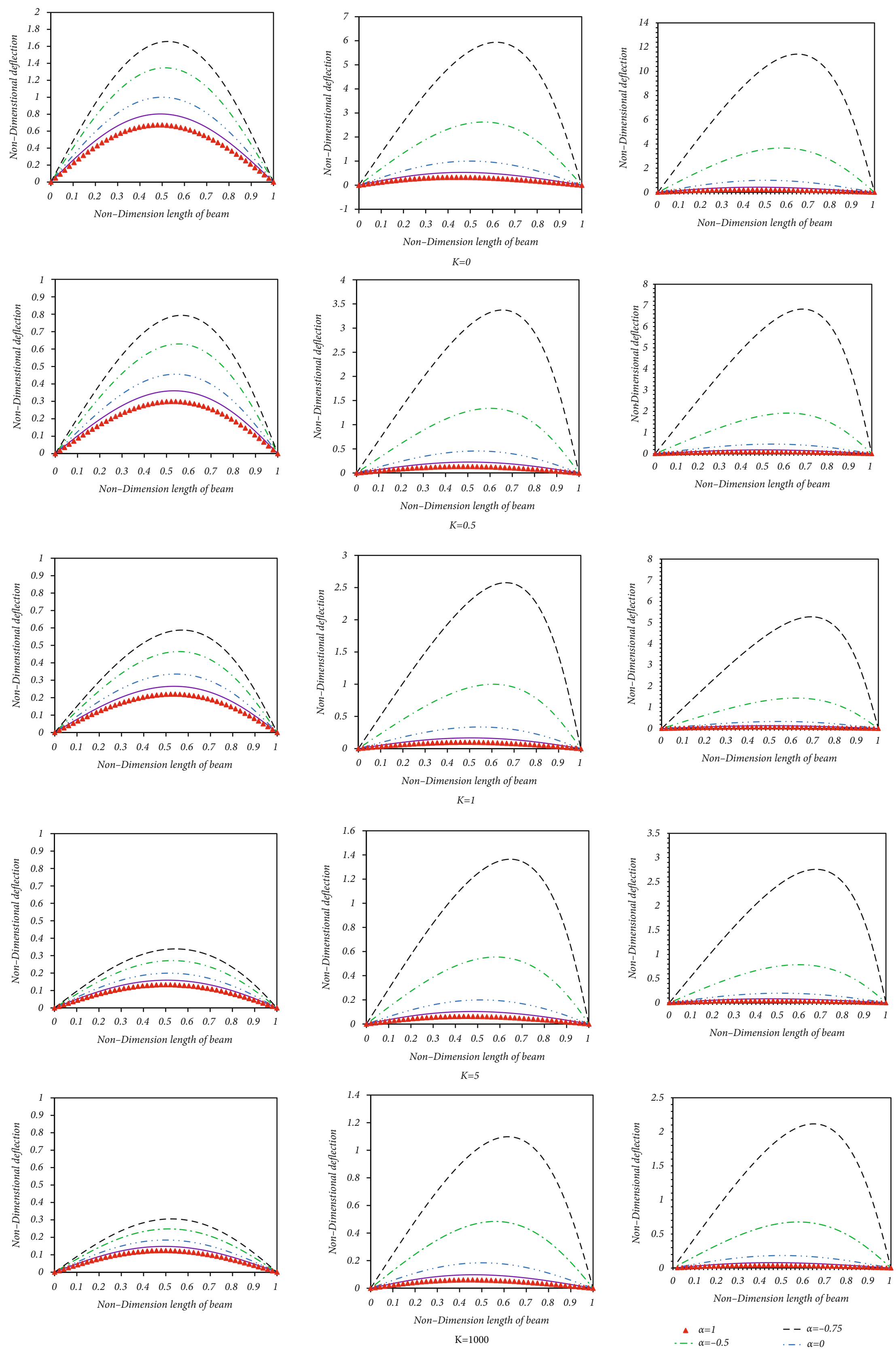

Figure 10: Static nondimensional deflection along the length of simply-supported A-FGB under distribution load with different non-uniformity parameters.

3.4. Path Results of Static Deflection. To extend the study, the effects of the power-law index (K) and non-uniformity parameters on the dimensionless deflection along the length of the free-clamped A-FGBs are shown in Figure 8. Generally, the width variation effects are not significant on the deflection in the beam in comparison with the thickness variation effects and the combination of both width and thickness variations, where it has the greater effects. In other words, the effects of variations mean that the dimensionless deflection increases as the non-uniformity parameters are reduced. It seems that increasing the rate of dimensionless deflection leads to an increase in decreasing the non-uniformity parameters.

However, the effects of thickness variation are larger as shown in Figure 9 for the clamped-free beam in comparison with the effects of changing the width of the beam.

For simply-supported A-FGB as shown in Figure 10, the effects of width variation, thickness variation, and both width and thickness variation cause to increase the dimensionless deflection, in addition to changing the position of maximum dimensionless deflection.

Generally, the mid-span is the position of the maximum deflection in a simply-supported beam (i.e., $x = l/2$). When both width and thickness are varied, the dimensionless deflections give the largest values compared with thickness and width variations alone. It seems that the position of dimensionless deflection is changed due to the variation in the dimensions of the beam and the distribution of elastic modulus.

4. Conclusions

The static analysis of non-prismatic A-FGB at different supporting types was carried out using the ANSYS workbench (17.2). The following conclusions can be drawn from the results.

The power-law index and non-uniformity parameters affect the maximum dimensionless deflection. In other words, with increasing the power-law index, the max-dimensionless deflection decreases at the same non-uniformity parameters, while the maximum dimensionless deflection decreases with increasing the non-uniformity parameters.

In free-clamped A-FGB, the effects of non-uniformity parameters are greater than that of the power-law index. The effects of variation of both width and thickness are significant on the dimensionless deflection of the beam compared with other variations.

In clamped-free A-FGB, the effects of thickness variation are notable compared with other variations.

In simply-supported A-FGB, the effects of variation of both width and thickness are significant compared with other variations.

Data Availability

Data is available upon request.

Conflicts of Interest

The authors declare that they have no conflicts of interest.

References

[1] W. S. Ebhota and T. C. Jen, “Casting and applications of functionally graded metal matrix composites,” *Advanced Casting Technologies*, vol. 59, 2018.

[2] S. Jamian, *Application of Functionally Graded Materials for Severe Plastic Deformation and Smart Materials : Experimental Study and Finite Element Analysis*, Doctoral dissertation, Nagoya Institute of Technology, 2012.

[3] R. Singh, V. Bhavar, P. Kattire, S. Thakare, S. Patil, and R. K. P. Singh, “A review on functionally gradient materials (FGMs) and their applications,” *Materials Science and Engineering*, vol. 229, no. 1, article 012021, 2017.

[4] M. R. Zarastvand, M. Ghassabi, and R. Talebitooti, “Acoustic insulation characteristics of shell structures: a review,” *Archives of Computational Methods in Engineering*, vol. 28, no. 2, pp. 505–523, 2021.

[5] A. A. Hendi, M. A. Eltaher, S. A. Mohamed, M. A. Attia, and A. W. Abdalla, “Nonlinear thermal vibration of pre/post-buckled two-dimensional FGM tapered microbeams based on a higher order shear deformation theory,” *Steel and Composite Structures*, vol. 41, no. 6, pp. 787–803, 2021.

[6] M. A. Eltaher, A. Wagih, A. Melaibari, G. S. Alsoruji, and M. A. Attia, “Elastoplastic indentation response of sigmoid/power functionally graded ceramics structures,” *Polymers*, vol. 14, no. 6, p. 1225, 2022.

[7] R. Talebitooti, M. Zarastvand, and H. Darvishgohari, “Multi-objective optimization approach on diffuse sound transmission through poroelastic composite sandwich structure,” *Journal of Sandwich Structures & Materials*, vol. 23, no. 4, pp. 1221–1252, 2021.

[8] M. H. Asadijafari, M. R. Zarastvand, and R. Talebitooti, “The effect of considering Pasternak elastic foundation on acoustic insulation of the finite doubly curved composite structures,” *Composite Structures*, vol. 256, article 113064, 2021.

[9] E. E. Ghandourah, H. M. Ahmed, M. A. Eltaher, M. A. Attia, and A. M. Abdraboh, “Free vibration of porous FG nonlocal modified couple nanobeams via a modified porosity model,” *Advances in Nano Research*, vol. 11, no. 4, pp. 405–422, 2021.

[10] M. Şimşek, “Static analysis of a functionally graded beam under a uniformly distributed load by Ritz method,” *International Journal of Engineering and Applied Sciences*, vol. 1, no. 3, pp. 1–11, 2009.

[11] H. Zhu and B. V. Sankar, “A combined Fourier series–Galerkin method for the analysis of functionally graded beams,” *Journal of Applied Mechanics*, vol. 71, no. 3, pp. 421–424, 2004.

[12] A. Chakraborty, S. Gopalakrishnan, and J. N. Reddy, “A new beam finite element for the analysis of functionally graded materials,” *International Journal of Mechanical Sciences*, vol. 45, no. 3, pp. 519–539, 2003.

[13] G. Baker, “On the large deflections of non-prismatic cantilevers with a finite depth,” *Computers and Structures*, vol. 46, no. 2, pp. 365–370, 1993.

[14] B. K. Lee, J. F. Wilson, and S. J. Oh, “Elastica of cantilevered beams with variable cross sections,” *International Journal of Non-Linear Mechanics*, vol. 28, no. 5, pp. 579–589, 1993.

[15] M. Brojan, T. Videnic, and F. Kosel, "Large deflections of nonlinearly elastic non-prismatic cantilever beams made from materials obeying the generalized Ludwick constitutive law," *Meccanica*, vol. 44, no. 6, pp. 733–739, 2009.

[16] R. Attarnejad, S. J. Semnani, and A. Shahba, "Basic displacement functions for free vibration analysis of non-prismatic Timoshenko beams," *Finite Elements in Analysis and Design*, vol. 46, no. 10, pp. 916–929, 2010.

[17] B. V. Sankar, "An elasticity solution for functionally graded beams," *Composites Science and Technology*, vol. 61, no. 5, pp. 689–696, 2001.

[18] R. Kadoli, K. Akhtar, and N. Ganesan, "Static analysis of functionally graded beams using higher order shear deformation theory," *Applied Mathematical Modelling*, vol. 32, no. 12, pp. 2509–2525, 2008.

[19] K. V. Singh and G. Li, "Buckling of functionally graded and elastically restrained non-uniform columns," *Composites Part B: Engineering*, vol. 40, no. 5, pp. 393–403, 2009.

[20] Y. A. Kang and X. F. Li, "Bending of functionally graded cantilever beam with power-law non-linearity subjected to an end force," *International Journal of Non-Linear Mechanics*, vol. 44, no. 6, pp. 696–703, 2009.

[21] Y. A. Kang and X. F. Li, "Large deflections of a non-linear cantilever functionally graded beam," *Journal of Reinforced Plastics and Composites*, vol. 29, no. 12, pp. 1761–1774, 2010.

[22] A. E. Alshorbagy, M. A. Eltaher, and F. F. Mahmoud, "Free vibration characteristics of a functionally graded beam by finite element method," *Applied Mathematical Modelling*, vol. 35, no. 1, pp. 412–425, 2011.

[23] N. Wattanasakulpong, B. G. Gangadhara, and D. W. Kelly, "Thermal buckling and elastic vibration of third-order shear deformable functionally graded beams," *International Journal of Mechanical Sciences*, vol. 53, no. 9, pp. 734–743, 2011.

[24] A. Shahba, R. Attarnejad, M. T. Marvi, and S. Hajilar, "Free vibration and stability analysis of axially functionally graded tapered Timoshenko beams with classical and non-classical boundary conditions," *Composites Part B: Engineering*, vol. 42, no. 4, pp. 801–808, 2011.

[25] J. R. Reddy, "On locking-free shear deformable beam finite elements," *Computer Methods in Applied Mechanics and Engineering*, vol. 149, no. 1–4, pp. 113–132, 1997.

[26] N.-T. Nguyen, N.-I. Kim, I. Cho, Q. T. Phung, and J. Lee, "Static analysis of transversely or axially functionally graded tapered beams," *Materials Research Innovations*, vol. 18, supplement 2, pp. S2-260–S2-264, 2014.

[27] N. D. Kien, "Large displacement response of tapered cantilever beams made of axially functionally graded material," *Composites: Part B*, vol. 55, pp. 298–305, 2013.

[28] S. N. Padhi, S. S. Choudhury, and T. Routyyynnn, "Static and dynamic stability analysis of a sigmoid functionally graded timoshenko beam," *International Journal of Advances in Mechanical and Civil Engineering*, vol. 2, no. 5, 2015.

[29] S. Rajasekaran and H. B. Khaniki, "Finite element static and dynamic analysis of axially functionally graded nonuniform small-scale beams based on nonlocal strain gradient theory," *Mechanics of Advanced Materials and Structures*, vol. 26, no. 14, pp. 1245–1259, 2019.

[30] Ş. D. Akbaş, "Post-buckling analysis of axially functionally graded three-dimensional beams," *International Journal of Applied Mechanics*, vol. 7, no. 3, article 1550047, 2015.

[31] D. L. Logan, *A "First Course in the Finite Element Method"*, Cengage Learning, 2016.

[32] ANSYS, *Mechanical APDL Element Reference*, ANSYS, Inc., 2016.

[33] *Help of ANSYS Workbench Version 17.2.*, NSYS, Inc., 2016.